

Effect of Biot/Squirt (BISQ) Media on Plane Strain Vibrations of Poroelastic solids

Manjula Ramagiri

Department of Mathematics, University Arts and Science College, Kakatiya University, Warangal, India

ABSTRACT: This paper deals with effect of Biot/squirt media on plane strain vibrations of poroelastic solids. The frequency equations for both pervious and impervious surfaces are obtained in the framework of Biot's theory of wave propagation in poroelastic solids. Frequency and attenuation is computed as a function of wavenumber and average characteristic squirt flow length. For illustration purpose, two poroelastic solids are considered. Of two poroelastic solids, one is sandstone saturated with kerosene and the other is sandstone saturated water are employed, and the results are presented graphically.

KEYWORDS: Poroelasticity, Biot/squirt (BISQ) model, plane strain vibrations, frequency, wavenumber, attenuation.

I. INTRODUCTION

The theory of poroelasticity is widely used today in many applications such as Seismology, Biomechanics, Civil Engineering, and Mechanical Engineering. Employing the Biot's theory [1], deflection of poroelastic plates is studied by Taber [2]. Edge waves in poroelastic plate under plane stress conditions are studied by Malla Reddy and Tajuddin [3]. In the said paper, the governing equations of plane stress problem in poroelastic solids are formulated. Malla Reddy and Tajuddin [4] investigated exact analysis of plane strain vibrations of thick-walled hollow poroelastic cylinders. Three dimensional vibration analysis of an infinite poroelastic plate immersed in an inviscid elastic plate is studied by Shah and Tajuddin [5]. The isotropic poroelastic solids are investigated in the framework of Biot's theory by several authors [6, 7, 8, 9]. In all the above papers, pores are assumed to have uniform geometry, which are not realistic. In the squirt flow, pore geometry is considered individually. The Biot flow and squirt flow are two important mechanisms of fluid flow in porous media. In Biot mechanism, the fluid is forced to participate in the solid motion by viscous friction and inertial coupling, whereas in the the squirt flow mechanism the fluid is squeezed out of thin pores deformed by a passing wave. Dvorkin et al offered a consistent Biot/Squirt (BISQ) model based on the one dimensional porous isotropic case by combining the two mechanisms of solid/fluid interaction [10]. Parra studied the transversely isotropic poroelastic wave equation including the Biot and the squirt mechanisms; theory applications [11]. Effects of the Biot and squirt flow coupling interaction on anisotropic elastic waves is investigated by Yang and Zhang [12]. They concluded that, the attenuation of quasi P-wave and quasi SV-wave are strongly depend on the permeability anisotropy and the attenuation behaviors at low and high frequencies is contrary each other. Yang and Zhang [13] studied poroelastic wave equation including the Biot/squirt mechanism and the solid/fluid coupling anisotropy. Yang and Chen [14] investigated BISQ model for fluid filled porous medium. The generalized BISQ wave equation based on the solid/fluid coupling anisotropy is studied by Yang DH and Yang KD [15]. Diallo and Appel [16] investigated acoustic wave propagation in saturated porous media: Reformulation of Biot/squirt flow theory. Seismic modeling in isotropic porous media based on BISQ model is studied by Meng QingSheng et al [17]. Wave propagation and the frequency domain Green's functions in viscoelastic Biot/Squirt (BISQ) media is investigated by Yang et al [18]. In the paper [18], the frequency domain Green's functions for viscoelastic BISQ media are derived based on the classical potential function methods. The S-waves are only affected by viscoelasticity, but not by squirt flow and the phase velocity, attenuation of fast P-waves are seriously influenced by both viscoelasticity and squirt flow. Chang et al [19] presented a viscoelastic Biot/Squirt model by introducing a viscoelastic stress strain constitutive relationship of solid phases and found that the viscoelastic property of rocks, not the squirt flow causes the dispersion and attenuation in the low frequency range. Differential form and numerical implementation of Biot's poroelasticity equations with squirt dissipation is investigated by Carcione and Gurevich [20]. To the best of author's knowledge, effect of Biot/squirt

International Journal of Innovative Research in Science, Engineering and Technology

(A High Impact Factor & UGC Approved Journal)

Website: www.ijirset.com

Vol. 6, Issue 9, September 2017

media on plane strain vibrations of poroelastic solids is not yet investigated. Therefore, in this paper the same is investigated in the framework of Biot's theory. Frequency equations are obtained for both pervious and impervious surfaces. Frequency and attenuation against the wavenumber and average characteristic squirt flow length are computed for two solids namely sandstone saturated with kerosene and sandstone saturated with water.

II. GOVERNING EQUATIONS AND SOLUTION OF THE PROBLEM

The equations of motion of a poroelastic solid [1, 10] in the presence of dissipation are

$$N\nabla^2 \vec{u} + (A + N)\nabla e + Q\nabla \varepsilon = \frac{\partial^2}{\partial t^2}(\rho_{11}\vec{u} + \rho_{12}\vec{U}) + b\frac{\partial}{\partial t}(\vec{u} - \vec{U}),$$

$$\nabla P_1 = \frac{\partial^2}{\partial t^2}(\rho_{12}\vec{u} + \rho_{22}\vec{U}) - b\frac{\partial}{\partial t}(\vec{u} - \vec{U}). \quad (1)$$

where ∇^2 is the Laplace operator, $\vec{u} = (u, v, w)$ and $\vec{U} = (U, V, W)$ are solid and fluid displacements, e and ε are the dilatations of solid and fluid respectively; the symbols A, N, Q, R are all poroelastic constants; P_1 is the fluid pressure[10]. The constitutive relations are given by

$$\sigma_{ij} = 2Ne_{ij} + (Ae + Q\varepsilon)\delta_{ij} \quad (i, j = x, z)$$

$$P_1 = -FS(\varepsilon + Me) \quad (2)$$

In eq. (2), e_{ij} 's, are the strain displacements, σ_{ij} 's are the solid stresses, δ_{ij} is the well known Kronecker delta function

F, S are the Biot flow and squirt flow. $M = \frac{\alpha - \phi}{\phi}$, ϕ is the porosity and $\alpha = (1 - (\frac{2}{3}\mu + \lambda)\frac{1}{K_s})$, $N = \mu$

$A - \frac{Q^2}{R} = \lambda$, where λ, μ are lame constants, K_s is the bulk modulus of solid, and F, S are given by[10]

$$F = \left(\frac{1}{K_f} + \frac{\alpha - \phi}{\phi} \frac{1}{K_s}\right)^{-1}, S = 1 - \frac{2J_1(\lambda_1 R_1)}{\lambda_1 R J_0(\lambda_1 R_1)} \text{ and } \lambda_1^2 = \frac{\rho_f \omega^2}{F} \left(\frac{\phi + \rho_a / \rho_f}{\phi} + \frac{i\eta\phi}{\rho_f \omega k_{11}}\right) \quad (3)$$

In eq. (3), K_f is the bulk modulus of fluid, ρ_{ij} are mass coefficients such that the sums $\rho_{11} + \rho_{12}$ and $\rho_{12} + \rho_{22}$ represents the mass of solid and fluid per unit volume of bulk material following [1]. Furthermore, the mass parameters obey the inequalities $\rho_{11} > 0, \rho_{12} \leq 0, \rho_{22} > 0, (\rho_{11}\rho_{22} - \rho_{12}^2) > 0$. The coefficient ρ_{12} is the mass coupling parameter between solid and fluid phases, while ρ_{11}, ρ_{22} satisfy the relations $\rho_{11} = (1 - \phi)\rho_s - \rho_{12}, \rho_{22} = \phi\rho_s - \rho_{12}, \rho_{12} = -\rho_a \cdot \rho_a$ is the additional coupling density[10], η is the viscosity, k_{11} is the permeability, ρ_f , and ρ_s are the densities of fluid and solid, J_0, J_1 are the Bessel functions of zero and first order respectively. The parameter R represents the average characteristic squirt flow length. Consider the plane strain vibrations in rectangular Cartesian coordinate axes are chosen such that x -axis is in the direction of propagation. Introducing displacement potential functions ϕ'_s and ψ'_s which are functions of x, y, t as follows

$$u = \frac{\partial \phi_1}{\partial x} - \frac{\partial \psi_1}{\partial z}, \quad w = \frac{\partial \phi_1}{\partial z} + \frac{\partial \psi_1}{\partial x} \quad U = \frac{\partial \phi_2}{\partial x} - \frac{\partial \psi_2}{\partial z}, \quad W = \frac{\partial \phi_2}{\partial z} + \frac{\partial \psi_2}{\partial x} \quad (4)$$

Substitution of eq. (4) into eq. (1) gives

International Journal of Innovative Research in Science, Engineering and Technology

(A High Impact Factor & UGC Approved Journal)

Website: www.ijirset.com

Vol. 6, Issue 9, September 2017

$$\begin{aligned}
 P\nabla^2\phi_1 + Q\nabla^2\phi_2 &= (\rho_{11}\ddot{\phi}_1 + \rho_{12}\ddot{\phi}_2) + b(\dot{\phi}_1 - \dot{\phi}_2), \\
 -(FSM\nabla^2\phi_1 + FS\nabla^2\phi_2) &= (\rho_{12}\ddot{\phi}_1 + \rho_{22}\ddot{\phi}_2) - b(\dot{\phi}_1 - \dot{\phi}_2), \\
 N\nabla^2\psi_1 &= (\rho_{11}\ddot{\psi}_1 + \rho_{12}\ddot{\psi}_2) + b(\dot{\psi}_1 - \dot{\psi}_2), \\
 0 &= (\rho_{12}\ddot{\psi}_1 + \rho_{22}\ddot{\psi}_2) - b(\dot{\psi}_1 - \dot{\psi}_2).
 \end{aligned} \tag{5}$$

In the above equations $P = A + 2N$, and dot over the quantity represents the partial differentiation with respect to time t . For the plane harmonic waves travelling in the x -direction, we have the potential functions as follows:

$$\phi_1 = F_1(z)e^{i(\omega t - kz)}, \quad \phi_2 = F_2(z)e^{i(\omega t - kz)}, \quad \psi_1 = G_1(z)e^{i(\omega t - kz)}, \quad \psi_2 = G_2(z)e^{i(\omega t - kz)}. \tag{6}$$

In eq. (6), k is the wavenumber, ω is the frequency of the wave. Substitution of $\phi_1, \phi_2, \psi_1, \psi_2$ into eqs. (5), gives

$$\begin{aligned}
 P(F_1'' - k^2F_1) + Q(F_2'' - k^2F_2) &= -\omega^2(M_{11}F_1 + M_{12}F_2), \\
 -(FSM(F_1'' - k^2F_1) + FS(F_2'' - k^2F_2)) &= -\omega^2(M_{12}F_1 + M_{22}F_2), \\
 N(G_1'' - k^2G_1) &= -\omega^2(M_{11}G_1 + M_{12}G_2), \\
 0 &= \omega^2(M_{12}G_1 + M_{22}G_2).
 \end{aligned} \tag{7}$$

Solving the first two equations of eq. (7), we obtain

$$F_2 = E_1^2 F_1'' - E_2^2 F_1, \tag{8}$$

$$\text{where } E_1^2 = \frac{-(PFS - FSMQ)}{\omega^2(FSM_{12} + QM_{22})}, \quad E_2^2 = \frac{\omega^2(QM_{12} - FSM_{11}) - k^2(PFS - FSMQ)}{\omega^2(FSM_{12} + QM_{22})}$$

Substituting F_2 into the first equation of eq. (7), we obtain

$$\begin{aligned}
 F^{IV}(PFS - FSMQ) + F_1''(-\omega^2(PM_{22} - QM_{12} + FSM_{11} + FSMM_{12}) + 2k^2(PFS - FSMQ)) \\
 + F_1(k^2\omega^2(PM_{22} - QM_{12} + FSM_{11} + FSMM_{12}) - k^4(PFS - FSMQ) - \omega^4(M_{11}M_{12} - M_{12}^2 \\
 + 2M_{11}M_{12}FSQ^{-1})) = 0.
 \end{aligned} \tag{9}$$

Here the velocities of dilatational waves of first and second kind are given by

$$\begin{aligned}
 \frac{1}{V_1^2} + \frac{1}{V_2^2} &= \frac{PM_{22} - QM_{12} + FSM_{11} + FSMM_{12}}{PFS - FSMQ}, \\
 \frac{1}{V_1^2 V_2^2} &= \frac{M_{11}M_{22} - M_{12}^2 + 2M_{11}M_{12}FSQ^{-1}}{PFS - FSMQ}.
 \end{aligned} \tag{10}$$

Solving the eq. (9), we obtain F_1, F_2 for ϕ_1, ϕ_2 . Similarly, we can obtain G_1, G_2 for ψ_1, ψ_2 . substituting these into eq. (6) we obtain

$$\begin{aligned}
 \phi_1 &= (A_1 \cosh(pz) + B_1 \sinh(pz) + A_2 \cosh(qz) + B_2 \sinh(qz))e^{i(\omega t - kz)}, \\
 \phi_2 &= (A_1\delta_1^2 \cosh(pz) + B_1\delta_1^2 \sinh(pz) + A_2\delta_2^2 \cosh(qz) + B_2\delta_2^2 \sinh(qz))e^{i(\omega t - kz)}
 \end{aligned}$$

$$\psi_1 = (B_3 \cosh(k\beta z) + A_3 \sinh(k\beta z))e^{i(\omega t - kz)}, \tag{11}$$

$$\psi_2 = -\frac{M_{12}}{M_{22}}\psi_1,$$

International Journal of Innovative Research in Science, Engineering and Technology

(A High Impact Factor & UGC Approved Journal)

Website: www.ijirset.com

Vol. 6, Issue 9, September 2017

Where

$$p = -k\left(\frac{C^2}{V_1^2} + 1\right)^{1/2}, \quad q = -k\left(\frac{C^2}{V_2^2} + 1\right)^{1/2}, \quad \beta = \left(1 - \frac{C^2}{V_3^2}\right)^{1/2} \quad (12)$$

In eq. (11) and (12), $A_1, A_2, B_1, B_2, A_3, B_3$ all constants. C is the phase velocity of the wave. V_1^2 and V_2^2 are the velocities of dilatational waves of first and second kind, V_3^2 is the shear wave velocity [1]. δ_1^2 and δ_2^2 are

$$\delta_1^2 = \frac{(PFS - FSMQ) + (QM_{12} - FSM_{11})V_1^2}{V_1^2(FSM_{12} + QM_{22})}, \quad \delta_2^2 = \text{similar expression as } \delta_1^2 \text{ with } V_1^2 \text{ replaced by } V_2^2 \text{ and}$$

$$M_{11} = \rho_{11} - i\omega^{-1}, \quad M_{12} = \rho_{12} + i\omega^{-1}, \quad M_{22} = \rho_{22} - i\omega^{-1}.$$

Substituting $\phi_1, \phi_2, \psi_1, \psi_2$ into the eq. (4), we obtain the displacements:

$$u = -ik(A_1 \cosh(pz) + B_1 \sinh(pz) + A_2 \cosh(qz) + B_2 \sinh(qz) - i\beta B_3 \sinh(k\beta z) - i\beta A_3 \cosh(k\beta z))e^{i(\omega t - kz)},$$

$$w = (A_1 p \sinh(pz) + B_1 p \cosh(pz) + A_2 q \sinh(qz) + B_2 q \cosh(qz) - ikB_3 \cosh(k\beta z) - ikA_3 \sinh(k\beta z))e^{i(\omega t - kz)}. \quad (13)$$

By substituting the displacements into eq. (2), the relevant stresses and fluid pressure are respectively, given by

$$\sigma_{xx} + P_1 = [A_1[2Np^2 + ((A - FSM) + (Q - FS)\delta_1^2)(p^2 - k^2)]\cosh(pz) + B_1[2Np^2 + ((A - FSM) + (Q - FS)\delta_1^2)(p^2 - k^2)]\sinh(pz) + A_2[2Nq^2 + ((A - FSM) + (Q - FS)\delta_2^2)(q^2 - k^2)]\cosh(qz) + B_2[2Nq^2 + ((A - FSM) + (Q - FS)\delta_2^2)(q^2 - k^2)]\sinh(qz) - 2Ni\beta k^2 B_3 \sinh(k\beta z) - 2Ni\beta k^2 A_3 \cosh(k\beta z)]e^{i(\omega t - kz)},$$

$$\sigma_{xz} = -Nik[2A_1 p \sinh(pz) + 2B_1 p \cosh(pz) + 2A_2 q \sinh(qz) + 2B_2 q \cosh(qz) - ikB_3(\beta^2 + 1)\cosh(k\beta z) - ikA_3(\beta^2 + 1)\sinh(k\beta z)]e^{i(\omega t - kz)},$$

$$P_1 = -[A_1(FSM + FS\delta_1^2)(p^2 - k^2)\cosh(pz) + B_1(FSM + FS\delta_1^2)(p^2 - k^2)\sinh(pz) + A_2(FSM + FS\delta_2^2)(q^2 - k^2)\cosh(qz) + B_2(FSM + FS\delta_2^2)(q^2 - k^2)\sinh(qz)]e^{i(\omega t - kz)},$$

$$\frac{\partial P_1}{\partial z} = -[A_1(FSM + FS\delta_1^2)p(p^2 - k^2)\sinh(pz) + B_1(FSM + FS\delta_1^2)p(p^2 - k^2)\cosh(pz) + A_2(FSM + FS\delta_2^2)q(q^2 - k^2)\sinh(qz) + B_2(FSM + FS\delta_2^2)q(q^2 - k^2)\cosh(qz)]e^{i(\omega t - kz)}. \quad (14)$$

III. BOUNDARY CONDITIONS AND FREQUENCY EQUATIONS

The boundary conditions to be satisfied are

$$\sigma_{zz} + P_1 = \sigma_{xz} = P_1 = 0 \quad \text{at } z = \pm\alpha \quad (\text{pervious surface}) \quad (15)$$

$$\sigma_{zz} + P_1 = \sigma_{xz} = \frac{\partial P_1}{\partial z} = 0 \quad \text{at } z = \pm\alpha \quad (\text{impervious surface}) \quad (16)$$

International Journal of Innovative Research in Science, Engineering and Technology

(A High Impact Factor & UGC Approved Journal)

Website: www.ijirset.com

Vol. 6, Issue 9, September 2017

Equations (15) result in a system of six homogeneous equations in $A_1, A_2, A_3, B_1, B_2, B_3$. For a nontrivial solution the coefficient matrix determinant is zero. According, we obtain the following frequency equation for a pervious surface:

$$|A_{ij}| = 0, \quad i, j = 1, 2, 3, 4, 5, 6. \quad (17)$$

In eq. (17), the elements A_{ij} are

$$\begin{aligned} A_{11} &= (2Np^2 + (A - FSM) + (Q - FS)\delta_1^2)(p^2 - k^2) \cosh(p\alpha), \\ A_{12} &= (2Np^2 + (A - FSM) + (Q - FS)\delta_1^2)(p^2 - k^2) \sinh(p\alpha), \\ A_{13} &= (2Nq^2 + (A - FSM) + (Q - FS)\delta_2^2)(q^2 - k^2) \cosh(q\alpha), \\ A_{14} &= (2Nq^2 + (A - FSM) + (Q - FS)\delta_2^2)(q^2 - k^2) \sinh(q\alpha), \\ A_{15} &= -2Ni\beta k^2 \sinh(k\beta\alpha), \quad A_{16} = -2Ni\beta k^2 \cosh(k\beta\alpha), \\ A_{21} &= A_{11}, \quad A_{22} = -A_{12}, \quad A_{23} = A_{13}, \quad A_{24} = -A_{14}, \quad A_{25} = A_{15}, \quad A_{26} = -A_{16}, \\ A_{31} &= 2Np \sinh(p\alpha), \quad A_{32} = 2Np \cosh(p\alpha), \quad A_{33} = 2Nq \sinh(q\alpha), \\ A_{34} &= 2Nq \cosh(q\alpha), \quad A_{35} = -ikN(\beta^2 + 1) \cosh(q\alpha), \quad A_{36} = -ikN(\beta^2 + 1) \sinh(q\alpha), \\ A_{41} &= -A_{31}, \quad A_{42} = A_{32}, \quad A_{43} = -A_{33}, \quad A_{44} = A_{34}, \quad A_{45} = -A_{35}, \quad A_{46} = A_{36}, \\ A_{51} &= (FSM + FS\delta_1^2)(p^2 - k^2) \cosh(p\alpha), \quad A_{52} = (FSM + FS\delta_1^2)(p^2 - k^2) \sinh(p\alpha), \\ A_{53} &= (FSM + FS\delta_2^2)(q^2 - k^2) \cosh(q\alpha), \quad A_{54} = (FSM + FS\delta_2^2)(q^2 - k^2) \sinh(q\alpha), \quad A_{55} = A_{56} = 0, \\ A_{61} &= A_{51}, \quad A_{62} = -A_{52}, \quad A_{63} = A_{53}, \quad A_{64} = -A_{54}, \quad A_{65} = A_{66} = 0. \end{aligned} \quad (18)$$

Arguing on similar lines, employing the boundary conditions eq. (16) frequency equation of an impervious surface is

$$|B_{ij}| = 0, \quad i, j = 1, 2, 3, 4, 5, 6, \quad (19)$$

where

$$\begin{aligned} B_{11} &= A_{11}, \quad B_{12} = A_{12}, \quad B_{13} = A_{13}, \quad B_{14} = A_{14}, \quad B_{15} = A_{15}, \quad B_{16} = A_{16}, \\ B_{21} &= A_{21}, \quad B_{22} = A_{22}, \quad B_{23} = A_{23}, \quad B_{24} = A_{24}, \quad B_{25} = A_{25}, \quad B_{26} = A_{26}, \\ B_{31} &= A_{31}, \quad B_{32} = A_{32}, \quad B_{33} = A_{33}, \quad B_{34} = A_{34}, \quad B_{35} = A_{35}, \quad B_{36} = A_{36}, \\ B_{41} &= A_{41}, \quad B_{42} = A_{42}, \quad B_{43} = A_{43}, \quad B_{44} = A_{44}, \quad B_{45} = A_{45}, \quad B_{46} = A_{46}, \\ B_{51} &= (FSM + FS\delta_1^2)p(p^2 - k^2) \sinh(p\alpha), \quad B_{52} = (FSM + FS\delta_1^2)p(p^2 - k^2) \cosh(p\alpha), \\ B_{53} &= (FSM + FS\delta_2^2)q(q^2 - k^2) \sinh(q\alpha), \quad B_{54} = (FSM + FS\delta_2^2)q(q^2 - k^2) \cosh(q\alpha), \\ B_{55} &= B_{56} = 0, \quad B_{61} = -B_{51}, \quad B_{62} = B_{52}, \quad B_{63} = -B_{53}, \quad B_{64} = B_{54}, \quad B_{65} = B_{66} = 0 \end{aligned} \quad (20)$$

In eq. (20), A_{ij} are defined in eq. (18)

IV. NUMERICAL RESULTS

The frequency equation (17) and (19) is investigated for particular solids namely sandstone saturated with kerosene is material-1 while sandstone saturated water is material-2 [20, 21, 22, 23]. The additional coupling parameter value is given in [10]. The parameter values are given in Table-1. The attenuation coefficient is given by [24].

International Journal of Innovative Research in Science, Engineering and Technology

(A High Impact Factor & UGC Approved Journal)

Website: www.ijirset.com

Vol. 6, Issue 9, September 2017

Table-I

Kerosene saturated sandstone	Water saturated sandstone
$A = 0.306 \times 10^{10} \text{ N / m}^2$	$A = 0.4436 \times 10^{10} \text{ N / m}^2$
$N = 0.2765 \times 10^{10} \text{ N / m}^2$	$N = 0.922 \times 10^{10} \text{ N / m}^2$
$Q = 0.07635 \times 10^{10} \text{ N / m}^2$	$Q = 0.013 \times 10^{10} \text{ N / m}^2$
$R = 0.0326 \times 10^{10} \text{ N / m}^2$	$R = 0.0637 \times 10^{10} \text{ N / m}^2$
$\rho_{11} = 1.926137 \times 10^3 \text{ kg / m}^3$	$\rho_{11} = 1.90302 \times 10^3 \text{ kg / m}^3$
$\rho_{12} = -0.00213 \times 10^3 \text{ kg / m}^3$	$\rho_{12} = 0$
$\rho_{22} = 0.21537 \times 10^3 \text{ kg / m}^3$	$\rho_{22} = 0.268 \times 10^3 \text{ kg / m}^3$
Bulk modulus, $K_s = 6\text{Gpa}$	Bulk modulus, $K_s = 50\text{Gpa}$
Bulk modulus, $K_f = 2.14\text{Gpa}$	Bulk modulus, $K_f = 2.25\text{Gpa}$
Porosity, $\phi = 0.26$	Porosity, $\phi = 0.2$
Permeability, $k_{11} = 290\text{mD}$	Permeability, $k_{11} = 200\text{mD}$
Density, $\rho_f = 1000\text{kg / m}^3$	Density, $\rho_f = 1040\text{kg / m}^3$
Density, $\rho_s = 2100\text{kg / m}^3$	Density, $\rho_s = 2650\text{kg / m}^3$
Viscosity, $\eta = 1.53 \text{ mPa}$	Viscosity, $\eta = 0.001\text{Pa s}$

Employing the material values in the frequency eqs. (17) and (19), we obtain an implicit relation between frequency and wavenumber at average characteristic squirt flow length 0.001, 0.003 and 0.005. Frequency and attenuation is computed as a function of wavenumber and average characteristic squirt flow length and the results are depicted in figure 1-6. In all the cases, curves are periodic in nature. Figure-1 show the plots of frequency against wavenumber at average characteristic squirt flow length 0.001 for both pervious and impervious surface. From this figure, it is clear that frequency of material-1 values of an impervious surface are greater than that of material-1 pervious surface. Figure-2 show the plots of frequency against wavenumber at average characteristic squirt flow length 0.003 for both pervious and impervious surface. From this figure, it is seen that frequency of material-1 values of pervious surface are greater than that of material-1 values of an impervious surface. Also it is observed that frequency of material-2 values of an impervious surface are greater than that of material-2 values of pervious surface. Figure-3 show the plots of frequency against wavenumber at average characteristic squirt flow length 0.005 for pervious and an impervious surface. From this figure, it is observed that frequency of material-1, 2 values of an impervious surface are greater than that of material-1, 2 values of pervious surface. Figure-4 show the plots of attenuation against wavenumber at average characteristic squirt flow length 0.001. From this figure it is seen that material-1 values of pervious surface are greater than that of material-1 of an impervious surfaces. Also it is seen that material-2 values of an impervious surface are greater than that of material -2 of pervious surface. Figure-5, 6 show the plots of attenuation against wavenumber at average characteristic squirt flow length 0.003 and 0.005. From this figure it is clear that material-1, 2 values of pervious surface are greater than that of material-1, 2 values of impervious surface. From figure-1, 2, 3 it is observed that as the wavenumber increases frequency decreases. Also from the figures- 4, 5, 6 it is clear that as the wavenumber increases attenuation increases. This influence is due to the presence of fluid part present in the materials.

International Journal of Innovative Research in Science, Engineering and Technology

(A High Impact Factor & UGC Approved Journal)

Website: www.ijirset.com

Vol. 6, Issue 9, September 2017

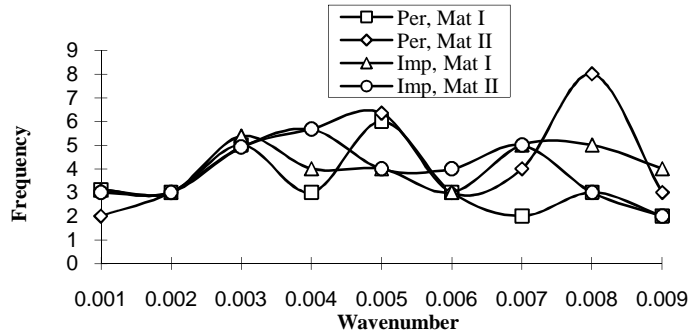


Fig-1 Variation of frequency with wavenumber at characteristic squirt flow length ($R_1 = 0.001$)

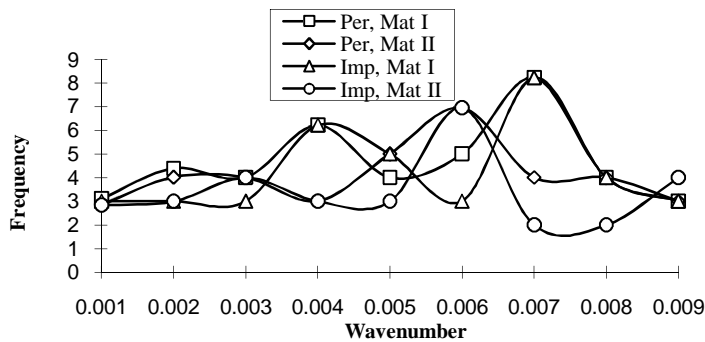


Fig-2 Variation of frequency with wavenumber at characteristic squirt flow length ($R_1 = 0.003$)

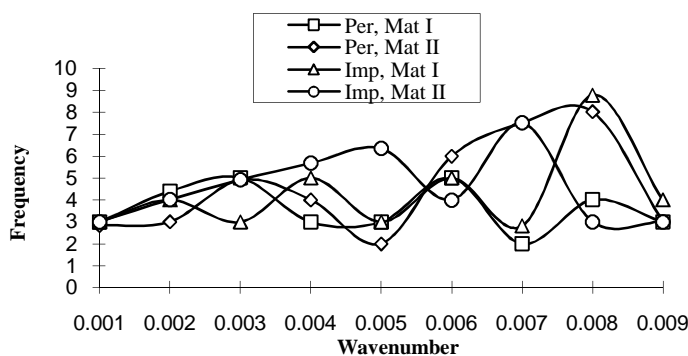


Fig-3 Variation of frequency with wavenumber at characteristic squirt flow length ($R_1 = 0.005$)

International Journal of Innovative Research in Science, Engineering and Technology

(A High Impact Factor & UGC Approved Journal)

Website: www.ijirset.com

Vol. 6, Issue 9, September 2017

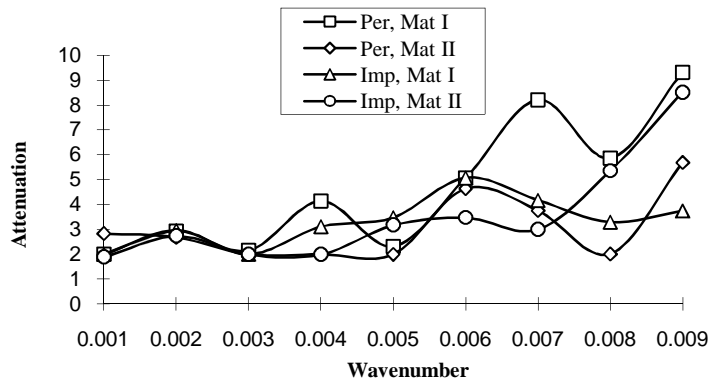


Fig-4 Variation of attenuation with wavenumber at characteristic squirt flow length ($R_1=0.001$)

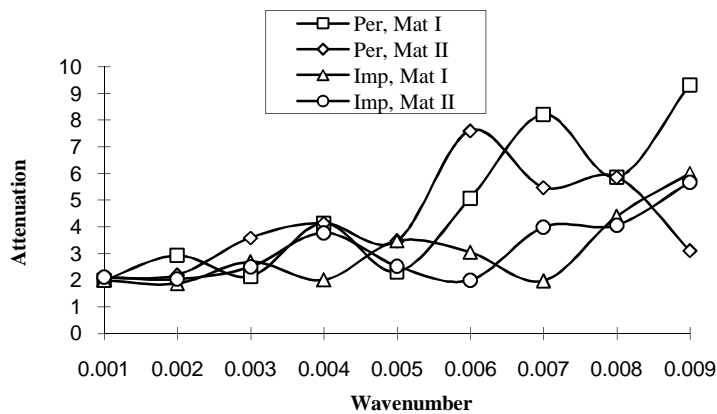


Fig-5 Variation of attenuation with wavenumber at characteristic squirt flow length ($R_1=0.003$)

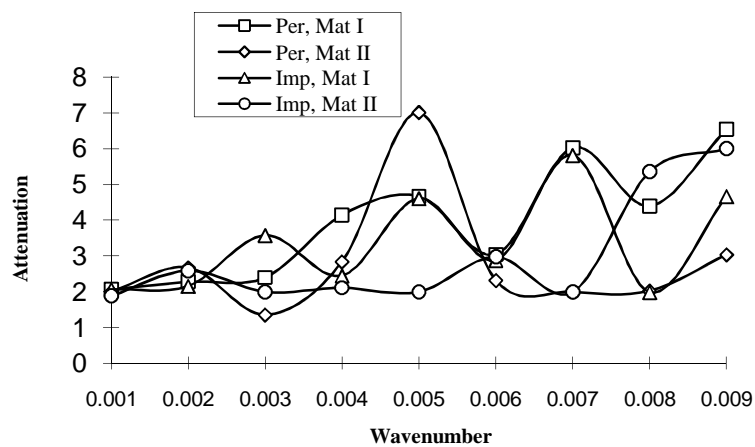


Fig-6 Variation of attenuation with wavenumber at characteristic squirt flow length ($R_1=0.005$)

International Journal of Innovative Research in Science, Engineering and Technology

(A High Impact Factor & UGC Approved Journal)

Website: www.ijirset.com

Vol. 6, Issue 9, September 2017

V. CONCLUSION

Effect of Biot/Squirt (BISQ) media on plane strain vibrations of poroelastic solids are investigated for both pervious and impervious surfaces. Frequency and attenuation is computed as a function of wavenumber and average characteristic squirt flow length. As the wavenumber increases frequency decreases and attenuation increases. This influence is due to the presence of fluid part and additional coupling parameter.

REFERENCES

- [1] Biot M.A, "The theory of propagation of elastic wave in fluid-saturated porous solid, Journal of the Acoustical Society of America", Vol. 28, pp.168-178, 1956.
- [2] Taber, "A theory for deflection of poroelastic plates", Journal of Applied Mechanics, Vol. 59, pp.628-634, 1960.
- [3] Malla Reddy P, Tajuddin M, "Edge waves in poroelastic plate under plane stress conditions", Journal of Acoustical Society of America, USA, 114(1), pp.185-193, 2003.
- [4] Malla Reddy, P. and Tajuddin M., "Exact analysis of the plane strain vibrations of thick walled hollow poroelastic cylinders", International Journal of Solids and Structures, Vol. 37, pp.3439-3456, 2000.
- [5] Shah and Tajuddin, "Three dimensional vibration analysis infinite poroelastic plate immersed in an inviscid elastic fluid", International Journal of Engineering Science and Technology, Vol. 30, pp.1-11, 2011.
- [6] Pradhan, Samal and Mahanti, "Shear waves in a fluid saturated elastic plate", Sadhana, Vol. 27, pp. 595-604, 2012.
- [7] Singh, Sarvajit, Rani, and Sunita, "Plane strain deformation of a multi layered poroelastic half space by surface loads", Journal of Earth System and Science, Vol.115(6), pp. 685, 2006.
- [8] Neelam Kumari and Assem Miglani, "Plane strain deformation of a poroelastic half space in welded contact with transversely isotropic elastic half space", International Journal of Engineering and Technology, Vol. 4(11), pp. 4555-4570, 2012.
- [9] Sandhya Rani, Malla Reddy and Gangadhar Reddy, "Dispersion study of plane strain vibrations in poroelastic solids bars with polygons cross section", Mathematics and Mechanics of solids, doi: 1177/1081286515571785, 2015.
- [10] Dvorkin J, Nur A, "Dynamic poroelasticity: A unified model with the Squirt and Biot mechanisms", Geophysics, Vol. 58(4), pp. 524-533, 1993.
- [11] Parra J O, "The transversely isotropic poroelastic wave equation including the Biot and the squirt mechanisms: Theory and application". Geophysics, Vol. 62(1), pp. 309-318, 1997.
- [12] Yang D H, Zhang Z J, "Effect of the Biot and the Squirt flow coupling interaction on anisotropic elastic waves", Chinese Science Bulletin, Vol. 45(230), pp.2130-2138, 2000.
- [13] Yang D H, Zhang Z J, "Poroelastic wave equation including the Biot/Squirt mechanism and solid/fluid coupling anisotropy", Wave Motion, Vol. 35(3), pp. 223-245, 2002.
- [14] Yang Dinghui, Chen Xiaohong, "BISQ model for fluid filled porous medium", OGP, 2001. 3692), PP. 146-159.
- [15] Yang D H, Yang K D, "The generalized BISQ wave equation based on the solid/fluid coupling anisotropy", SEG Technical Expanded Abstracts, Vol. 22, pp. 1306-1309, 2003.
- [16] Diallo M S, Appel E, "Acoustic wave propagation in saturated porous media: Reformulation of Biot/ Squirt flow theory", Journal of Applied Geophysics, Vol. 44(4), pp. 313-315, 2000.
- [17] Meng Qingsheng, He Qiaodeng and Zhu Jianwei, "Seismic modeling in isotropic porous media based on BISQ model", Journal of Jilin University (Earth Science Edition), Vol. 33(2), pp. 217-221, 2003.
- [18] Dinghui Yang, Yiqing Shen and Enru Liu, "Wave propagation and the frequency domain green's functions in viscoelastic Biot/ squirt (BISQ) media", International Journal of Solids and Structures, Vol. 44, pp. 4784-4794, 2007.
- [19] Cheng Y F, Yang D H and Yang H Z, "Biot/ Squirt model in viscoelastic porous media", Chinese Physics Letters, Vol. 19, pp. 445-448, 2002.
- [20] Jose M. Carcione, Boris Gurevich, "Differential form and numerical implementation of Biot's poroelasticity equations with squirt dissipation", Geophysics, Vol. 76(6), pp. 55-64, 2011.
- [21] Yew, C.H, and Jogi, P.N, "Study of wave motions in fluid-saturated porous rocks", Journal of the Acoustical Society of America, Vol. 60, pp.2-8, 1976.
- [22] Fatt I, "The Biot-Willis elastic coefficient for a sand stone", Journal Applied Mechanics, pp.296-297, 1957.
- [23] Nandal J S, Saini T N, "Effect of crack dilatancy on Rayleigh waves in fluid saturated porous media", International Journal of Engineering Science and Technology, Vol. 6(1), pp. 77-87, 2014.
- [24] Solorza and Sahay PN, "Standing torsional waves in a fully saturated porous circular cylinder", Geophysical Journal International, Vol.157, pp. 455-473, 2004.